J. Fluid Mech. (2008), *vol.* 608, *pp.* 379–391.
doi:10.1017/S0022112008002437 Printed in the United Kingdom

Mechanism of the long-wave inertialess instability of a two-layer film flow

PENG GAO AND XI-YUN LU†

Department of Modern Mechanics, University of Science and Technology of China, Hefei, Anhui 230026, China

(Received 27 January 2008 and in revised form 6 May 2008)

This paper provides an intuitive interpretation of the long-wave inertialess instability of a two-layer film flow. The underlying mechanism is elucidated by inspecting the longitudinal perturbation velocity associated with the surface and interfacial deflections. The velocity is expressed by the composition of three parts, related to the shear stress at the free surface, the continuity condition at the interface, and the pressure disturbance induced by gravity. The effect of each velocity component on the evolutions of the surface and the interface is examined in detail. Specifically, the growth of the free surface is caused by the continuity-induced first-order velocity disturbance associated with an additional phase shift between the surface and interfacial waves, while the growth of the interface is due to the pressure-driven flow. The proposed mechanism gives an alternatively reliable prediction of the wave velocity and growth rate.

1. Introduction

The stability of multiple-layer film flows with a free surface is of considerable interest since these flows occur in many industrial and engineering applications, such as coating in photography (Weinstein & Ruschak 2004). Owing to the gravity-driven flow down an inclined plane, multilayered films can give rise to instabilities in the form of travelling surface and interfacial waves, resulting in undesirable variations of film thicknesses. Thus, it is of significant importance to study the stability of such flows as well as the underlying mechanisms.

A linear stability of two-layer film flows was first studied by Kao, who employed a long-wave approximation to the Orr–Sommerfeld equation to resolve the stability of the flow with density stratification (Kao 1965*a*, *b*), and subsequently extended the work by including the effect of viscosity stratification (Kao 1968). He found that there existed two competing travelling-wave modes, usually termed the surface mode and the interface mode in later studies, responsible for the stability. Generally, the interface mode dominates and can lead to an unstable flow at zero Reynolds number. Since the instability associated with the interfacial mode does not rely on fluid inertia, it is referred to as inertialess instability. Loewenherz & Lawrence (1989) carried out a finite-wavelength stability analysis of the flow with matched densities as well as negligible surface/interfacial tension and fluid inertia, focusing primarily on the role of viscosity stratification. Their results showed that the inertialess instability occurs when the fluid in the upper layer is more viscous than the lower layer, and the most dangerous mode has a finite wavelength comparable with the film thickness; in

† Author to whom correspondence should be addressed: xlu@ustc.edu.cn

contrast, the flow configuration with the more viscous layer adjacent to the wall is stable for all wavenumbers. Chen (1993) considered the stability of the two-layer flow with the influence of inertia by numerically solving the Orr–Sommerfeld equation for finite Reynolds numbers, and found that the flow can only be stable when the inertial effect is small enough. In addition, he also demonstrated that the role of uniform surface and interfacial tensions is stabilizing for finite-wavelength disturbances and negligible for long waves. If the surface and interfacial tensions are modified by the presence of insoluble surfactants, the inertialess instability can be significantly weakened or enhanced (Gao & Lu 2007). By extending the work of Loewenherz & Lawrence (1989), Hu *et al.* (2006) performed a spatio-temporal stability analysis of the flow with combined effects of density and viscosity stratification, again for disturbances with finite wavelength and in the limit of Stokes flow.

Similar inertialess instability has also been encountered in film flows with a configuration of more than two layers. In this situation, there are several modes with the number equal to the number of the interfaces and one mode associated with the presence of the free surface. Wang, Seaborg & Lin (1978) formulated the problem of the stability of a general n-layer liquid film flow and specifically performed a long-wave stability analysis of a five-layer film. They found that the inertialess instability can occur in a flow with a downward step decrease in viscosity. A linear stability of a three-layer film in the limit of long waves was investigated by Weinstein & Kurz (1991). The growth of long waves is associated with the presence of complex conjugate wave velocities, which occur when the internal layer is relatively thin, and can persist into the finite wavelength domain (Weinstein & Chen 1999). The growth rates of the interfacial waves are much larger than those in two-layer film. The origin and evolution of the inertialess instability of a three-layer film were examined by Jiang *et al.* (2005) using analytical, numerical and experimental techniques. In particular, they performed an energy analysis and revealed the important role of the interfacial shear on the instability. Weakly nonlinear evolutions of the inertialess instability of three-layer flows have been studied by Kliakhandler & Sivashinsky (1997) and Kliakhandler (1999).

Although the inertialess instability of multiple-layer films has been extensively studied, the underlying mechanism seems not to have been completely elucidated. Chen (1993) conjectured that the inertialess instability of a two-layer film results from a kind of resonance between the free surface and the interface. This is reasonable since the inertialess instability does not occur when the interface is absent, corresponding to a single-layer falling film (Benjamin 1957; Yih 1963), or when the free surface is replaced with a rigid plate, corresponding to a two-layer channel flow (Yih 1967; Renardy 1985). However, the details of the resonance are still unclear. For the energy budget, Jiang, Helenbrook & Lin (2004) found that the inertialess instability of a two-layer film is caused by the interfacial shear work, though the origin of the work was not addressed. Huang & Khomami (2001) mentioned that the combined effects of the hydrostatic pressure and the disturbance vorticity lead to the instability; the interpretation seems to be inconsistent and questionable.

The primary purpose of this paper is to provide an intuitive and complete interpretation of the mechanism of the inertialess instability. We focus mainly on two-layer film flows because of their simplicity and rich dynamics. For convenience, only long waves will be considered here, allowing us to grasp the essential mechanism.

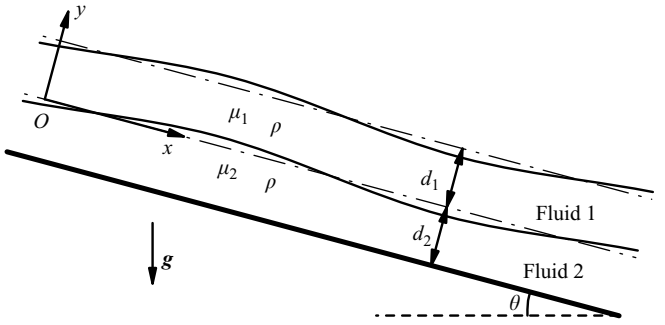

FIGURE 1. Schematic illustration of the two-layer flow down an inclined plane.

2. Long-wave instability mechanism of a two-layer film

2.1. *Problem statement and the basic flow*

Consider the gravity-driven film flow of two-fluid layers down an inclined plane which is tilted at an angle θ with respect to the horizontal direction. The flow configuration and the coordinate system are shown in figure 1. The fluids are assumed to be incompressible and Newtonian. The upper layer is occupied by fluid 1 with mean thickness d_1 and dynamic viscosity μ_1, and the lower layer by fluid 2 with mean thickness d_2 and viscosity μ_2. For simplicity, we assume that the two fluids have the same density ρ. To non-dimensionalize the system, we use d_2 as the scale of length, and define the characteristic velocity as

$$\hat{U} = \rho g d_2^2 \sin\theta/\mu_2,$$

where g is the acceleration due to gravity. The time and pressure are scaled by $d_2/\hat{U}$ and $\mu_2\hat{U}/d_2$, respectively. Then, the dimensionless forms of the basic velocity profile and the pressure distribution are

$$U_1(y) = m^{-1}\left(\delta y - \tfrac{1}{2}y^2\right) + \delta + \tfrac{1}{2}, \tag{2.1a}$$

$$U_2(y) = \delta y - \tfrac{1}{2}y^2 + \delta + \tfrac{1}{2}, \tag{2.1b}$$

$$P_1(y) = P_2(y) = (\delta - y)\cot\theta, \tag{2.1c}$$

where m and δ are, respectively, the ratios of viscosities and thicknesses of the two layers, defined by

$$m = \frac{\mu_1}{\mu_2}, \quad \delta = \frac{d_1}{d_2}.$$

2.2. *Disturbances of the flow field*

We introduce infinitesimally small velocity perturbations $u_j(x, y, t)$, $v_j(x, y, t)$ and pressure perturbations $p_j(x, y, t)$ for $j = 1, 2$, and let $h_1(x, t)$ and $h_2(x, t)$ denote the departures of the perturbed free surface and fluid–fluid interface from their mean locations. Further, we focus on long-wave perturbations associated with the inertialess instability, i.e. the wavenumber $k \ll 1$ and the fluid inertia being negligible. These assumptions allow us to identify each factor leading to the disturbance flow field and to consider the relevant contributions to the instability. The longitudinal velocity perturbations u_j can be divided into three parts, related to the shear stress at

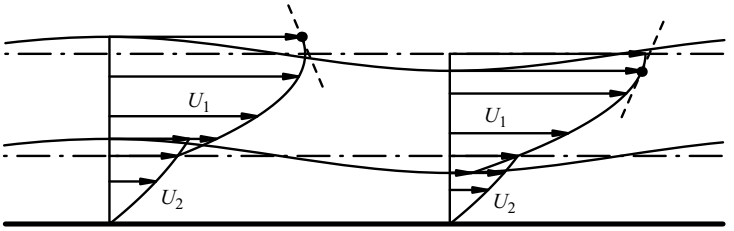

FIGURE 2. Sketch illustrating the non-zero shear at the perturbed free surface and the discontinuity at the perturbed interface of the basic velocity profile for $m < 1$. The dashed lines indicate the slope of the velocity profile at the free surface.

the free surface, the continuity condition at the interface and the pressure disturbance induced by gravity, which will be described below.

A constraint for free-surface film flows is that the shear stress at the surface vanishes. At the perturbed free surface with a displacement h_1, the shear stress of the basic flow (2.1a) is non-zero owing to the curvature of the basic velocity profile, as shown in figure 2. Thus, a perturbation shear stress, equal to $-U_1''(\delta)h_1$, develops to satisfy the free-surface condition. This viewpoint was also discussed by Kelly *et al.* (1989) and Smith (1990) in explaining the instability mechanism of a single-fluid film flow. For Stokes flow and long waves, the perturbation shear stress drives a linear shear flow, $u^{(s)}$, in both fluid layers,

$$u_1^{(s)} = -U_1''(\delta)h_1(y+m) = \left(\frac{y}{m}+1\right)h_1, \tag{2.2a}$$

$$u_2^{(s)} = -mU_1''(\delta)h_1(y+1) = (y+1)h_1. \tag{2.2b}$$

The profile of this perturbation flow field is shown in figure 3(a). Note that the slope difference of $u^{(s)}$ is due to the viscosity stratification of the two layers, and figure 3(a) shows the case of $m < 1$.

At the perturbed interface $y = h_2$, the velocity of the two fluids must be continuous. However, the basic velocities of the two layers are not continuous owning to the viscosity stratification of the flow (see also figure 2). As a result, an additional disturbance flow, denoted by $u^{(c)}$, arises to make the overall velocity continuous at the interface. Taking into account the no-slip condition at the wall and the zero-shear condition at the free surface, the disturbance velocities resulting from the continuity condition have the form

$$u_1^{(c)} = [U_2'(0) - U_1'(0)]h_2 = \delta\left(1-\frac{1}{m}\right)h_2, \tag{2.3a}$$

$$u_2^{(c)} = 0. \tag{2.3b}$$

It can be seen that this flow occurs only in the upper fluid and remains uniform across the layer. The velocity $u^{(c)}$ is different from the counterpart of a two-layer channel flow, in which the continuity-induced disturbance flow is linear in both fluids at the leading order (Charru & Hinch 2000) owing to the no-slip conditions at the two walls. A typical profile of $u^{(c)}$ for $m < 1$ is shown in figure 3(b), while the velocity for $m > 1$ is reversed.

The third part of the disturbance velocity is related to the presence of a gravity component perpendicular to the wall, which, together with a perturbed free surface, causes a hydrostatic pressure disturbance $p_1 = p_2 = p \equiv h_1 \cot\theta$ in both fluids. Note

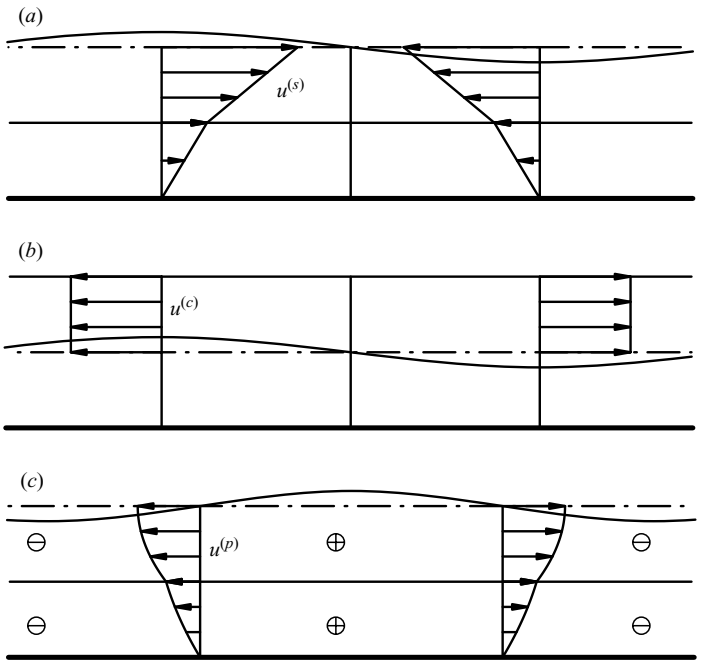

FIGURE 3. The longitudinal velocities for $m < 1$ generated by (a) the perturbation shear stress at the free surface, (b) the continuity of velocity at the perturbed interface, and (c) the disturbance pressure p. The regions of $p > 0$ and $p < 0$ are indicated by $\oplus$ and $\ominus$, respectively.

that the pressure disturbance is constant in the y-coordinate and slowly varying in the x-coordinate since only long waves and matched densities are considered. The pressure is in phase with the surface deflection; that is, as shown in figure 3(c), the pressure distribution attains its maximum (or minimum) under the crest (or trough) of the surface wave. As a result, a parabolic flow, $u^{(p)}$, will be driven by the pressure gradient $\partial p/\partial x$ and reads

$$u_1^{(p)} = \left(\frac{1}{2m}y^2 - \frac{\delta}{m}y - \delta - \frac{1}{2}\right)\frac{\partial h_1}{\partial x}\cot\theta, \tag{2.4a}$$

$$u_2^{(p)} = \left(\frac{1}{2}y^2 - \delta y - \delta - \frac{1}{2}\right)\frac{\partial h_1}{\partial x}\cot\theta. \tag{2.4b}$$

Note that the magnitude of $u^{(p)}$ is $O(k)$ higher than those of $u^{(s)}$ and $u^{(c)}$. This pressure-driven flow serves to push the fluid away from the crest to the trough of the free surface in both the layers, and hence tends to stabilize the surface. The effect of $u^{(p)}$ on the growth of the interface depends on the phase difference between the surface and interfacial waves, and will be discussed later.

In view of (2.2)–(2.4), the total velocity disturbances,

$$u_j = u_j^{(s)} + u_j^{(c)} + u_j^{(p)}, \tag{2.5}$$

are directly expressed in terms of the qualities associated with the surface and interfacial deflections. The disturbance flow field may alternatively be obtained by solving the Stokes equation similarly to Wei (2005), but it is difficult to identify the individual flow components.

2.3. *Normal-mode solutions of disturbances*

To satisfy the mass conservation in both fluid layers, the velocity fields derived above will lead to wave motions and exponential growth of the free surface and the interface. We consider the normal-mode form of the surface and interfacial deflections,

$$h_1(x,t) = \tilde{h}_1 \cos[k(x-ct)] \exp(k^2\sigma t), \tag{2.6a}$$

$$h_2(x,t) = \tilde{h}_2 \cos[k(x-ct-\varphi)] \exp(k^2\sigma t), \tag{2.6b}$$

where k is the wavenumber and is assumed to be small for long waves as mentioned earlier, c is the wave velocity, $k\varphi$ is the phase shift of $O(k)$, and $s = k^2\sigma$ is the growth rate of disturbances, which is expected to be $O(k^2)$ according to Kao (1968). The normal-mode form of the velocity components can be easily obtained according to (2.2)–(2.4).

The unknowns in (2.6) can be determined by analysing the mass conservation in the control volumes V1: $[0 \leqslant x \leqslant \lambda/2,\ -1 \leqslant y \leqslant \delta + h_1]$ and V2: $[0 \leqslant x \leqslant \lambda/2,\ -1 \leqslant y \leqslant h_2]$, with $\lambda = 2\pi/k$ being the wavelength, according to

$$\frac{\mathrm{d}V_j}{\mathrm{d}t} + Q_j^{net\_out} = 0, \quad (j = 1, 2), \tag{2.7}$$

where V_j denotes the time-dependent volume of Vj and $Q_j^{net\_out}$ is the net volume flux leaving the control volume. Take the control volume V1 as an example,

$$V_1 = \int_0^{\lambda/2} (1 + h_2)\, \mathrm{d}x, \quad Q_1^{net\_out} = \int_{-1}^{h_2} (U_2 + u_2)\, \mathrm{d}y \Big|_{x=0}^{\lambda/2}. \tag{2.8}$$

Upon substituting the corresponding qualities into (2.7) and neglecting terms of $O(k^2)$, we obtain,

$$\begin{aligned} &\left[\tfrac{1}{2}\tilde{h}_1 + (U_I - c)\tilde{h}_2\right] \cos(kct) \\ &\quad = k\left[\left(\tfrac{1}{2}\delta + \tfrac{1}{3}\right)\tilde{h}_1 \cot\theta + \sigma\tilde{h}_2 + \varphi(U_I - c)\tilde{h}_2\right] \sin(kct), \end{aligned} \tag{2.9a}$$

$$\begin{aligned} &\left[(2U_S - c)\tilde{h}_1 + \delta^2\left(1 - \frac{1}{m}\right)\tilde{h}_2\right] \cos(kct) \\ &\quad = k\left[\left(\frac{\delta^3}{3m} + \delta^2 + \delta + \tfrac{1}{3}\right)\tilde{h}_1 \cot\theta + \sigma\tilde{h}_1 + \delta^2\left(1 - \frac{1}{m}\right)\varphi\tilde{h}_2\right] \sin(kct), \end{aligned} \tag{2.9b}$$

where

$$U_S = \frac{\delta^2}{2m} + \delta + \tfrac{1}{2}, \qquad U_I = \delta + \tfrac{1}{2}, \tag{2.10}$$

are the basic surface and interfacial velocities, respectively. To assure the validation of (2.9) at arbitrary time t, the four coefficients of $\cos(kct)$ and $\sin(kct)$ must vanish. We thus arrive at four equations, with two of them written in matrix form as

$$\begin{bmatrix} 2U_S & \delta^2\left(1 - \dfrac{1}{m}\right) \\ \tfrac{1}{2} & U_I \end{bmatrix} \begin{bmatrix} \tilde{h}_1 \\ \tilde{h}_2 \end{bmatrix} = c \begin{bmatrix} \tilde{h}_1 \\ \tilde{h}_2 \end{bmatrix}, \tag{2.11}$$

and the other two as

$$\begin{bmatrix} \tilde{h}_2/\tilde{h}_1 & (U_I - c)\tilde{h}_2/\tilde{h}_1 \\ 1 & \delta^2\left(1 - \dfrac{1}{m}\right)\tilde{h}_2/\tilde{h}_1 \end{bmatrix} \begin{bmatrix} \sigma \\ \varphi \end{bmatrix} = - \begin{bmatrix} \left(\tfrac{1}{2}\delta + \tfrac{1}{3}\right)\cot\theta \\ \left(\dfrac{\delta^3}{3m} + \delta^2 + \delta + \tfrac{1}{3}\right)\cot\theta \end{bmatrix}. \tag{2.12}$$

Based on these equations, the unknown qualities of the normal modes can be readily obtained. Obviously, (2.11) and (2.12) are decoupled, and hence the phase velocity c can be solved separately from (2.11). Note that this convenience is attributed to the long-wave approximations, under which the travelling-wave motions and the growth of perturbations can be separated; for finite-wavelength perturbations, we have to return to solve a more general eigenvalue problem with a strong coupling between the phase velocity and the growth rate.

System (2.11) is merely an eigenvalue problem with the phase velocity c being the eigenvalue and $[\tilde{h}_1, \tilde{h}_2]^T$ the eigenfunction. After some manipulations, the two eigenvalues can be written as

$$c^{\pm} = U_S + \tfrac{1}{2}U_I \pm \frac{K}{4m}, \tag{2.13}$$

where

$$K = \sqrt{4\delta^4 + 4m\delta^2(2\delta - 1) + m^2(12\delta^2 + 4\delta + 1)}.$$

The two normal modes associated with c^+ and c^- are, respectively, referred to as 'surface mode' and 'interface mode', corresponding to travelling surface and interfacial waves. In a reference moving downstream with velocity $U_S + U_I/2$, the surface-mode waves will propagate downward and the interface-mode waves propagate upward with the same phase velocity $K/4m$. The eigenfunctions associated with the surface and interface modes are

$$\left(\frac{\tilde{h}_2}{\tilde{h}_1}\right)^+ = \frac{2m}{m + 2m\delta + 2\delta^2 + K}, \tag{2.14a}$$

$$\left(\frac{\tilde{h}_2}{\tilde{h}_1}\right)^- = \frac{m + 2m\delta + 2\delta^2 + K}{4(1-m)\delta^2}. \tag{2.14b}$$

The values of σ and φ corresponding to the modes can be expressed in terms of c and $\tilde{h}_2/\tilde{h}_1$ according to the linear system (2.12). Substitution of (2.13) and (2.14) yields two groups of solutions, i.e.

$$\sigma^+ = -\frac{J}{6m}\cot\theta, \tag{2.15a}$$

$$\varphi^+ = \frac{\delta(1+\delta)(m + 3m\delta + 2\delta^2)^2(m + 2m\delta + 2\delta^2 + K)}{3JK^2}\cot\theta, \tag{2.15b}$$

for the surface mode, and

$$\sigma^- = \frac{2\delta^3(m-1)(1+\delta)(m + 3m\delta + 2\delta^2)^2}{3JK^2}\cot\theta, \tag{2.16a}$$

$$\varphi^- = \frac{2J}{3(m + 2m\delta + 2\delta^2 + K)}\cot\theta, \tag{2.16b}$$

for the interface mode. Here

$$J = m + 3m\delta + 3m\delta^2 + \delta^3 + K^{-1}[2\delta^5 + m\delta^2(8\delta^2 + \delta - 2) + m^2(12\delta^3 + 13\delta^2 + 5\delta + 1)].$$

The phase velocities and growth rates derived above are in exact agreement with the long-wave results of Kao (1968) in the absence of density stratification. Compared with Kao (1968), the results in the present paper have the advantage that the stability characteristics of the flow can be readily identified just from inspecting the formulations, instead of presenting a series of figures.

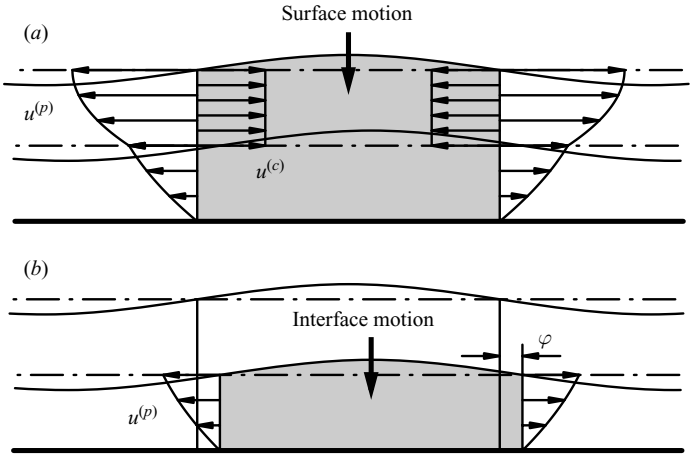

FIGURE 4. Stability diagram when the surface and interfacial waves are nearly in phase, corresponding to the surface mode for all m and the interface mode for $m < 1$. (a) The combined effects of $u^{(p)}$ and $\Delta u^{(c)}$ result in a downward motion of the surface crest. Note that the profile of $\Delta u^{(c)}$ is for $m < 1$, whereas the velocity is reversed for $m > 1$. (b) The pressure-driven velocity $u^{(p)}$ leads to a downward motion of the interfacial crest.

The stability or instability of the flow is determined by the sign of σ. It can be proved that for the parameters considered ($\delta > 0$, $m > 0$), the values of K and J are always positive. Thus, the surface mode is stable since the corresponding growth rate, $k^2\sigma$, is always negative in view of (2.15a). The associated surface and interfacial waves are in phase at the leading order according to (2.14a). Different from the surface mode, (2.16a) shows that the stability of the interface mode depends on the sign of $m - 1$. When the lower layer is more (or less) viscous, i.e. $m < 1$ (or $m > 1$), the growth rate of the interface mode is negative (or positive) and hence the mode is stable (or unstable). At the leading order, the corresponding surface and interfacial waves are in phase for the stable case, similar to the surface mode, and are out of phase by π for the unstable case, as indicated by (2.14b).

2.4. *Instability mechanism*

The evolution of small disturbances can be divided into a travelling-wave motion and a growth motion, similar to Smith (1990) and Charru & Hinch (2000). It is of interest to investigate the detailed instability mechanism, especially the contribution of each velocity component presented in §2.2 to the surface and interfacial growth.

Since φ is non-zero, the phase difference between the surface and interfacial waves are not exactly in phase or out of phase by π up to the $O(k)$ approximation. It is helpful to approximate the interfacial deflection h_2 as

$$h_2 \approx \bar{h}_2 + \Delta h_2, \tag{2.17a}$$

with

$$\bar{h}_2 = \tilde{h}_2 \cos[k(x - ct)] \exp(k^2\sigma t), \tag{2.17b}$$

$$\Delta h_2 = k\varphi\tilde{h}_2 \sin[k(x - ct)] \exp(k^2\sigma t), \tag{2.17c}$$

according to (2.6b). In fact, $\bar{h}_2$ is the leading-order position of the interface and Δh_2 is a correction of $O(k)$. Physically, the effect of Δh_2 can also be equivalently regarded as a shift of the interface related to its leading-order position, and the physical meaning of φ is the translational distance of the interface, as indicated in figures 4(b) and 5(b).

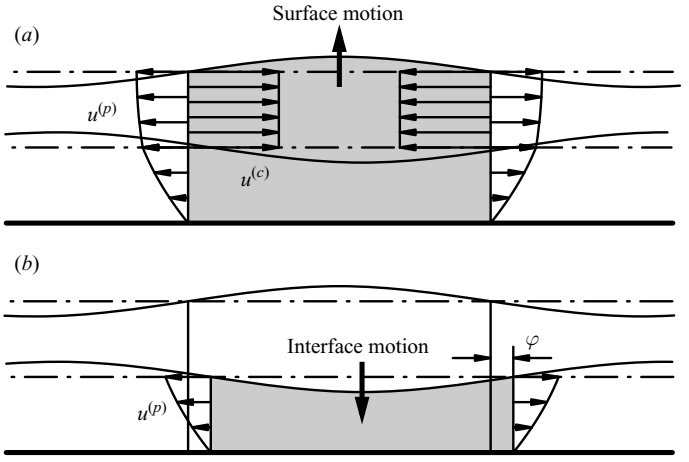

FIGURE 5. Stability diagram when the surface and interfacial waves are nearly out of phase by π, corresponding to the interface mode for $m > 1$. (*a*) The combined effects of $u^{(p)}$ and $\Delta u^{(c)}$ result in an upward motion of the surface crest. (*b*) The pressure-driven velocity $u^{(p)}$ leads to a downward motion of the interfacial trough.

Note that the interfacial wave is always shifted downstream since φ is always positive in view of (2.15*b*) and (2.16*b*). By substituting (2.17) into (2.3), the velocity field due to the continuity condition at the interface, $u^{(c)}$, can also be decomposed as

$$u^{(c)} \approx \bar{u}^{(c)} + \Delta u^{(c)}. \tag{2.18}$$

The expressions of $\bar{u}^{(c)}$ and $\Delta u^{(c)}$ are similar to (2.3) except that h_2 is replaced with $\bar{h}_2$ and Δh_2, respectively. In particular,

$$\Delta u_1^{(c)} = \delta \left(1 - \frac{1}{m}\right) \Delta h_2, \tag{2.19a}$$

$$\Delta u_2^{(c)} = 0. \tag{2.19b}$$

Obviously, $\Delta u^{(c)}$ is of $O(k)$, and attains its maximum at the midpoints of the surface and interfacial waves.

The mechanism of the travelling-wave motions of the surface and interface is relatively simple; it is caused by the leading-order perturbation velocities, i.e. $u^{(s)}$ and $\bar{u}^{(c)}$. The magnitudes of $u^{(s)}$ and $\bar{u}^{(c)}$ attain their maxima under the crest or trough of the surface and the interface, and vanish at the midpoints. The volume fluxes induced by the leading-order velocities are thus balanced by a shift of the surface and the interface, resulting in motions of perturbations in the form of travelling waves, as is well known. By applying the mass conservation condition (2.7) to the control volumes V1 and V2 and considering only the influences of $u^{(s)}$ and $\bar{u}^{(c)}$, we can simply obtain trivial solutions of the growth rates, while the eigenvalue problem (2.11) gives the phase velocities and the amplitude ratios of the deflections.

The growth of the surface and interfacial waves is induced by the first-order flows, i.e. the pressure-driven velocity $u^{(p)}$ and the velocity correction $\Delta u^{(c)}$ associated with the presence of the interfacial shift φ. According to the linear stability results, the surface and interfacial waves are stable (or unstable) when the leading-order phase difference between them is zero (or π). This conclusion is valid for both the surface

mode and the interface mode. We thus discuss the growth mechanism by considering separately the stable case and the unstable case rather than the two modes.

First we consider the stable case, in which the surface and interfacial waves are nearly in phase, as shown in figure 4. This case corresponds to the surface mode for all m and the interface mode for $m < 1$. To study the evolution of the surface and interface, we investigate the mass conservation of fluids in two control volumes denoted by the grey areas in figure 4. Note that these control volumes are different from V1 and V2 defined above, and have the advantage that the net fluxes due to the basic velocity profile vanish, since the edges of the control volumes correspond to the midpoints of the surface and interfacial waves. As shown in figure 4(a), the pressure-drive flow, $u^{(p)}$, moves fluid away from the surface crests and towards the surface troughs in both fluid layers, and hence plays a stabilizing role in the surface deformation. The effect of $\Delta u^{(c)}$ depends on the viscosity ratio m. When the lower fluid is more viscous ($m < 1$), the velocity $\Delta u^{(c)}$ drives the fluid in the upper layer away from the trough to the crest of the surface and hence tends to stimulate the surface growth, in contrast to the pressure-driven flow. However, this growth is not greater than the surface decay caused by the disturbance pressure and so the flow is stable. When the lower fluid is less viscous ($m > 1$), the velocity of $\Delta u^{(c)}$ shown in figure 4(a) is reversed; the in-phase configuration is now related just to the surface mode. Clearly, both $\Delta u^{(c)}$ and $u^{(p)}$ give rise to a downward motion of the surface crest and are stabilizing. The decay mechanism of the interface is shown in figure 4(b). Within the control volume considered, the pressure-driven flow $u^{(p)}$ produces a loss of mass, which is balanced by a decrease of the interfacial deformation. Note that $\Delta u^{(c)}$ does not directly contribute to the motion of the interface, since it occurs only in the upper layer.

The unstable case corresponds to the interface mode for $m > 1$ and can be similarly explained. The surface and interfacial waves are out of phase at the leading order, as shown in figure 5. The effect of the pressure-driven flow on the free surface is again stabilizing since $u^{(p)}$ corresponds to fluid motions from the trough to the crest of the surface. On the contrary, the flow of $\Delta u^{(c)}$ tends to destabilize the free surface. Different from the stable case, this destabilizing effect is strong enough to compete with the pressure-induced surface decay and leads to a net upward motion of the surface crest, corresponding to an increase of the surface deformation (figure 5a). The disturbance pressure in the lower layer is positive (or negative) around the regions under the interfacial trough (or crest). Therefore, the produced flow $u^{(p)}$ is now related to fluid motions in the lower layer from the trough to the crest of the interface, as shown in figure 5(b), leading to a downward motion of the interfacial trough. Thus, the pressure-driven flow plays a destabilizing influence on the interfacial wave and the interface deformation is also amplified.

3. Concluding remarks

We have provided an explanation of the underlying mechanism for the long-wave inertialess instability of a two-layer film flow by extending the work of Smith (1990) for a single-layer film and of Charru & Hinch (2000) for a two-layer channel flow. Mechanisms of both the surface and interface modes are interpreted in the same framework. The initiating mechanism is associated with the fact that the basic velocities do not satisfy the zero-shear condition at the perturbed free surface and the continuity condition at the perturbed interface. When the surface is disturbed, a disturbance shear stress develops and drives a linear longitudinal flow in both fluids. In

addition, to maintain the continuity of the fluids at the deformed interface, a uniform flow in the upper layer must occur. At the leading order, the influence of these flows is to induce the travelling-wave motions of the surface and interface to ensure mass conservation. The propagations of the surface and interfacial waves depend on each other, and they are either in phase or out of phase by π at the leading order.

The growth mechanism of the inertialess instability is associated with a pressure-driven flow and an extra phase shift between the surface and the interface. The component of gravity perpendicular to the wall induces a disturbance pressure field, which is uniform across both the layers and slowly varying in the longitudinal direction. The flow driven by this pressure acts to reduce the surface deformation, reflecting the well-known stabilizing effect of gravity. The same effect also holds on the interface when it is in phase with the surface at the leading order. When the surface and interface are out of phase at the leading order, the pressure-driven flow has a destabilizing influence on the interfacial wave, opposite to that on the surface wave. However, the instability cannot be completely explained by considering only the disturbance pressure. In the upper layer, the interfacial shift φ produces a first-order flow $\Delta u^{(c)}$, which, together with the pressure-driven flow, gives rise to the exponential growth of both the surface and the interface. The stability or instability can again be identified from mass conservation. In particular, for the interfacial mode at $m > 1$, the phase-shift-induced flow tends to destabilize the free surface, overwhelming the stabilizing effect of gravity. Note that the importance of the additional phase shift of the interface on the instability seems to have been overlooked in previous studies. The presented mechanisms not only serve as a complete physical interpretation, but also provide an alternative way of predicting the growth rates and wave velocities, complementing previous linear analyses (e.g. Kao 1968; Loewenherz & Lawrence 1989).

In contrast to the two-layer film flow, a single-layer falling film is stable at zero Reynolds number. Physically, as in the two-layer film, the decay of the free surface is due to the stabilizing effect of the normal component of gravity (Smith 1990). This stabilizing effect dominates the stability of the single-layer film, since there is a lack of mechanism to generate a flow exciting the surface growth when inertia is negligible. If the free surface of the two-layer film is replaced with a rigid wall, we obtain a two-layer channel flow, which is neutral in the limit of Stokes flow. The instability of this flow relies on the fluid inertia and the occurrence of lubrication pressure, and is independent of gravity (e.g. Yih 1967; Charru & Hinch 2000); the instability mechanism is quite different from the counterpart in the two-layer film.

The contribution of the pressure disturbances to the inertialess instability of a two-layer falling film was also mentioned by Huang & Khomami (2001); however, their interpretation seems to be questionable. In particular, the pressure was predicted to attain its maximum under the trough of the free surface for $m > 1$. More importantly, it is impossible to give a reasonable explanation of the growth of the free surface for $m > 1$ by considering only the pressure-driven flow. Based on the present analysis, this inconsistency is overwhelmed by the presence of an additional first-order flow, associated with the fact that the surface and interfacial waves are not exactly in phase or out of phase by π. The combined influence of the pressure-driven flow and this additional flow can make the surface and interfacial waves evolve with identical growth rates, which is of interest in the linear stability based on normal modes. The requirement of identical growth rates for both the waves in the two-layer film is similar to the constraint of no net mass flux for the disturbances in a two-layer pipe or channel flow, which is satisfied by the development of lubrication pressure (Smith 1989; Charru & Hinch 2000; Wei 2005). However, owing to the presence of the free

surface of the two-layer film, no such mechanism exists to induce lubrication pressure. Alternatively, the constraint is satisfied by the development of an additional phase shift of the surface and the interface, as discussed above. Note that the equality of growth rates of the surface and the interface is not necessarily true in general, but it is true for normal modes under consideration here.

Finally, although only two-layer film flows have been considered in the present study, we anticipate that the proposed mechanism should be quite common and can be extended to film flows with configuration of more than two layers, in which inertialess instability has been widely detected (Wang *et al.* 1978; Weinstein & Kurz 1991; Weinstein & Chen 1999). In addition, the mechanism of the instability of an oscillatory film with or without surfactants (Yih 1968; Gao & Lu 2006, 2008) can be interpreted in a similar way.

This work was supported by the Innovation Funds of Graduates at USTC, the National Natural Science Foundation of China (nos. 90405007 and 90605005), Program for Changjiang Scholars and Innovative Research Team in University, and the Fund for Foreign Scholars in University Research and Teaching Programs. The authors thank the referees for their valuable comments.

REFERENCES

Benjamin, T. B. 1957 Wave formation in laminar flow down an inclined plane. *J. Fluid Mech.* **2**, 554–574.

Charru, F. & Hinch, E. J. 2000 'Phase diagram' of interfacial instabilities in a two-layer Couette flow and mechanism of the long-wave instability. *J. Fluid Mech.* **414**, 195–223.

Chen, K. P. 1993 Wave formation in the gravity-driven low-Reynolds number flow of two fluid films down an inclined plane. *Phys. Fluids* A **5**, 3038–3048.

Gao, P. & Lu, X.-Y. 2006 Effect of surfactants on the long-wave stability of oscillatory film flow. *J. Fluid Mech.* **562**, 345–354.

Gao, P. & Lu, X.-Y. 2007 Effect of surfactants on the inertialess instability of a two-layer film flow. *J. Fluid Mech.* **591**, 495–507.

Gao, P. & Lu, X.-Y. 2008 Instability of an oscillatory fluid layer with insoluble surfactants. *J. Fluid Mech.* **595**, 461–490.

Hu, J., Millet, S., Botton, V., Hadid, H. B. & Henry, D. 2006 Inertialess temporal and spatio-temporal stability analysis of the two-layer film flow with density stratification. *Phys. Fluids* **18**, 104101.

Huang, C. T. & Khomami, B. 2001 The instability mechanism of single and multilayer Newtonian and viscoelastic flows down an inclined plane. *Rheol. Acta* **40**, 467–484.

Jiang, W. Y., Helenbrook, B. & Lin, S. P. 2004 Inertialess instability of a two-layer liquid film flow. *Phys. Fluids* **16**, 652–663.

Jiang, W. Y., Helenbrook, B. T., Lin, S. P. & Weinstein, S. J. 2005 Low-Reynolds-number instabilities in three-layer flow down an inclined wall. *J. Fluid Mech.* **539**, 387–416.

Kao, T. W. 1965*a* Stability of two-layer viscous stratified flow down an inclined plane. *Phys. Fluids* **8**, 812–820.

Kao, T. W. 1965*b* Role of the interface in the stability of stratified flow down an inclined plane. *Phys. Fluids* **8**, 2190–2194.

Kao, T. W. 1968 Role of viscosity stratification in the stability of two-layer flow down an incline. *J. Fluid Mech.* **33**, 561–572.

Kelly, R. E., Goussis, D. A., Lin, S. P. & Hsu, F. K. 1989 The mechanism for surface wave instability in film flow down an inclined plane. *Phys. Fluids* A **1**, 819–828.

Kliakhandler, I. L. 1999 Long interfacial waves in multilayer thin films and coupled Kuramoto–Sivashinsky equations. *J. Fluid Mech.* **391**, 45–65.

Kliakhandler, I. L. & Sivashinsky, G. I. 1997 Viscous damping and instabilities in stratified liquid film flowing down a slightly inclined plane. *Phys. Fluids* **9**, 23–30.

Loewenherz, D. S. & Lawrence, C. J. 1989 The effect of viscosity stratification on the stability of a free surface flow at low Reynolds number. *Phys. Fluids* A **1**, 1686–1693.

Renardy, Y. 1985 Instability at the interface between two shearing fluids in a channel. *Phys. Fluids* **28**, 3441–3443.

Smith, M. K. 1989 The axisymmetric long-wave instability of a concentric two-phase pipe flow. *Phys. Fluids* A **1**, 494–506.

Smith, M. K. 1990 The mechanism for the long-wave instability in thin liquid films. *J. Fluid Mech.* **217**, 469–485.

Wang, C. K., Seaborg, J. J. & Lin, S. P. 1978 Instability of multi-layered liquid films. *Phys. Fluids* **21**, 1669–1673.

Wei, H.-H. 2005 On the flow-induced Marangoni instability due to the presence of surfactant. *J. Fluid Mech.* **544**, 173–200.

Weinstein, S. J. & Chen, K. P. 1999 Large growth rate instabilities in three-layer flow down an incline in the limit of zero Reynolds number. *Phys. Fluids* **11**, 3270–3282.

Weinstein, S. J. & Kurz, M. R. 1991 Long-wavelength instabilities in three-layer flow down an incline. *Phys. Fluids* A **3**, 2680–2687.

Weinstein, S. J. & Ruschak, K. J. 2004 Coating flows. *Annu. Rev. Fluid Mech.* **36**, 29–53.

Yih, C. S. 1963 Stability of liquid flow down an inclined plane. *Phys. Fluids* **6**, 321–334.

Yih, C. S. 1967 Instability due to viscosity stratification. *J. Fluid Mech.* **27**, 337–352.

Yih, C. S. 1968 Instability of unsteady flows or configurations. Part 1. Instability of a horizontal liquid layer on an oscillating plane. *J. Fluid Mech.* **31**, 737–751.